ZnO/graphene heterostructure nanohybrids for optoelectronics and sensors

Judy Wu and Maogang Gong

View Online   Export Citation   CrossMark

ARTICLES YOU MAY BE INTERESTED IN

ZnO/graphene heterostructure nanohybrids for optoelectronics and sensors

View Online   Export Citation   CrossMark

Judy Wu[a)] and Maogang Gong[b)]

AFFILIATIONS

Department of Physics and Astronomy, University of Kansas, Lawrence, Kansas 66045, USA

[a)]E-mail: jwu@ku.edu
[b)]Author to whom correspondence should be addressed: gmg@ku.edu

ABSTRACT

The discovery of graphene has prompted an intensive exploration and research of heterostructure nanohybrids that integrate functionalities of semiconductor nanostructures with graphene's high charge carrier mobility, extraordinary mechanical strength, and flexibility for various applications. Among others, zinc oxide (ZnO) presents a promising candidate due to its unique physical properties including direct bandgap in ultraviolet spectrum, ferroelectricity, and hence piezoelectricity, moderate Debye length for electron depletion effect in ZnO nanostructures (quantum dots, nanowire, nanoparticles), etc. For ZnO/graphene heterostructure nanohybrids, the low thermal budget for growth of crystalline ZnO makes it possible for direct deposition of ZnO on graphene with controlled morphology and interface, enabling a large spectrum of devices including photodetectors, gas sensors, strain sensors, and self-power devices. In this Perspective, we discuss the recent progress made in ZnO/graphene heterostructure nanohybrids through understanding and engineering the ZnO/graphene interface to realize high performance. An overview of the remaining issues and future perspectives toward commercialization of the ZnO/graphene heterostructure nanohybrids will also be provided.

I. INTRODUCTION AND BACKGROUND

Graphene—a monolayer of carbon atoms arranged in two-dimensional hexagonal lattice of only 0.34 nm in thickness—has attracted extensive interest during the past decade or so due to its superior physical properties including high charge carrier mobility, optical transparency, mechanical strength, flexibility, and chemical stability.[1,2] Graphene may be viewed as an atomically thin film available in large area[3] and is compatible with conventional thin film-based microelectronics since the established microfabrication processes can be readily applied to make graphene-based electronic, photonic, and optoelectronic devices and circuits. These unique advantages have motivated explorations of various graphene-based applications[4–6] especially heterostructure nanohybrids consisting of graphene and other semiconductor nanostructures of different morphologies of 0D (quantum dots, nanocrystals, and nanoparticles),[4,7–10] 1D (nanotubes and nanowires),[11,12] and 2D (nanosheets of 2D atomic materials, thin films).[5,13,14] The implementation of graphene makes a fundamental difference in the charge carrier transport in these nanohybrids devices as compared to the counterparts based on the nanostructures due to the extraordinary charge carrier mobility in

graphene when it is used as the charge transport channel for signals. Among others, zinc oxide (ZnO) nanostructures are particularly suitable for nanohybrids with graphene, as we shall detail later, because of not only its interesting physical properties but also its compatibility of growth conditions for generation of various functional heterostructure nanohybrids on graphene. Due to the excellent properties of graphene and ZnO, both have been widely investigated for applications including high-performance graphene field effect transistors (GFETs),[15,16] optoelectronic devices,[17,18] chemical and strain sensors,[19,20] lasers,[21,22] and piezoelectronic nanogenerators.[23,24] The ZnO/graphene heterostructure nanohybrids integrate the physical properties of the graphene and ZnO, providing a unique platform for exploration of a wide variety of applications ranging from photodetectors,[9,25–34] gas sensors,[35–39] and stress/strain sensors.[31,40–42] Figure 1 highlights a few representative functional device applications based on ZnO/graphene heterostructure nanohybrids. The appeal of the ZnO/graphene heterostructure nanohybrids for these applications is that they combine the advantages of ZnO as a wide direct bandgap semiconductor, piezoelectric, biocompatible, and inexpensive, and graphene
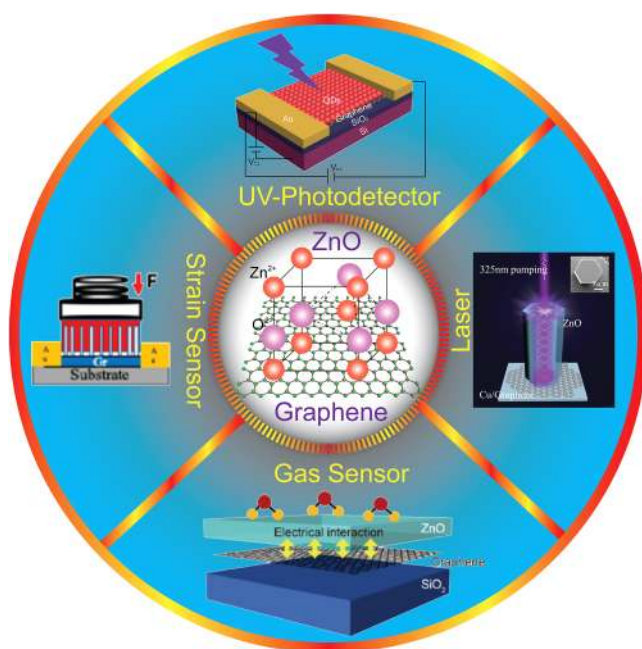
FIG. 1. Schematic scheme of the ZnO/graphene hybrid heterostructure for various functional device applications. Reproduced with permission from Gong et al., ACS Nano **11**, 4114 (2017). Copyright 2017 American Chemical Society; Panth et al., ACS Appl. Nano Mater. **3**, 6711 (2020). Copyright 2020 American Chemical Society; Qin et al., J. Mater. Chem. C **6**, 3240 (2018). Copyright 2018 The Royal Society of Chemistry; Bae et al., ACS Appl. Mater. Interfaces **11**, 16830 (2019). Copyright 2019 American Chemical Society.

as a flexible, conductive sheet of high charge mobility, transparent, and environmentally stable and chemically inert.[43–46]

A. Graphene

Graphene has attracted broad research interest due to its unique properties, such as ultrahigh carrier mobility, chemical and mechanical stability, excellent optical transparency, and good mechanical strength and elasticity.[10,47,48] Intrinsic graphene has a zero bandgap $E_g = 0$ as its conduction and valance bands join at the so-called Dirac point.[49] This would prohibit its use in a similar way to semiconductors of finite E_g values. Therefore, graphene absorbs incident light via interband transitions and exhibits a flat absorption $A = \pi\alpha \approx 2.3\%$ or transmittance $T = 1\text{-}A = 97.7\%$ (the fine-structure constant $\alpha = e^2/(4\pi\varepsilon_0\hbar c) = G_0/(\pi\varepsilon_0 c) \approx 1/137$) per graphene sheet in broadband from near ultraviolet (UV) to mid-infrared.[50–52] Graphene is a relativistic semiconductor (or semimetal) and its electronic structure can be described by a linear dispersion of $E = \hbar v_F k$.[52] The electrons and holes are therefore massless fermions with momentum-independent Fermi velocity v_F as high as 1/300 of the speed of light. This results in high carrier mobility (μ) that seems independent of temperature in a large range, independent of the applied electric field, and is comparable for holes and electrons.[49] The intrinsic acoustic phonon limit

of graphene's mobility is projected to be ∼200 000 cm²/V s at room temperature assuming a carrier density of $(n) \sim 10^{12}\,\text{cm}^{-2}$ at the charge neutrality or the so-called Dirac point.[49,53] Experimentally, high μ in the range of 1000–20 000 cm²/V s has been reported on graphene for both electrons and holes at room temperature, which could be further improved by eliminating extrinsic charge scatting mechanisms and defects in graphene.[54,55] It should be pointed out that the carrier mobility in graphene is significantly higher than that in metals and most semiconductors. For example, crystalline Si has the electron mobility of ∼1400 cm²/V s at room temperature.[56] The high μ in graphene means high electric conductivity can be obtained even at low carrier concentration at $n \sim 10^{12}/\text{cm}^2$ for intrinsic graphene. The low n (keep in mind the frequency cutoff that determines the transparency window is proportional to n[57,58]) and high conductivity make graphene an excellent alternative[6] to conventional transparent conductors[59] broadly employed for a large variety of photonic and optoelectronic applications.[14,54] In addition, graphene has additional advantages of flexibility, low cost, light weight, and a favorable work function of ∼4.42 eV comparable to many metals.[6,60–64]

B. ZnO

ZnO is a wide-bandgap semiconductor in the II–VI semiconductor group.[65–68] ZnO has a relatively large direct bandgap of 3.2–3.4 eV in UV spectrum and high exciton binding energy (60 meV) at room temperature.[65,69,70] The bandgap of ZnO can be tunable with elemental substitution on both the cation (Zn) and anion (O) sites. ZnO is typically n-type due to native doping by zinc interstitials and oxygen vacancies. Controllable n-doping by substitution of Zn with group III elements of Al, Ga, In, etc. allows enhancement of electrical conductivity of ZnO for transparent conductor applications of ZnO thin and thick films as well as nanostructures. ZnO is non-toxic, earth-abundant, and low cost and has been widely used in electronics, optoelectronics, cosmetics, food, adhesives, cement, and lubricants.

ZnO crystallizes into two main forms, hexagonal wurtzite and cubic zincblende.[68,71] The wurtzite structure is more stable at ambient conditions and thus most common. The zincblende form can be stabilized by growing ZnO on substrates with cubic lattice structure. Hexagonal and zincblende polymorphs have no inversion symmetry (reflection of a crystal relative to any given points does not transform it into itself). These ZnO lattice symmetry properties result in ferroelectricity as well as piezoelectricity of hexagonal and zincblende ZnO,[72,73] and pyroelectricity of hexagonal ZnO.[74,75] Various synthesis methods have been developed. Thin films can be produced by chemical vapor deposition (CVD), metal organic vapor phase epitaxy, electrodeposition, pulsed laser deposition, sputtering, sol-gel synthesis, atomic layer deposition (ALD), spray pyrolysis, etc. Nanostructures can be obtained mostly using the above-mentioned techniques at certain conditions and also with the vapor–liquid–solid method.[22,40,41] The solution-processed ZnO synthesis is typically carried out at a temperature of about 90 °C, in an equimolar aqueous solution of zinc nitrate and hexamine, the latter providing the basic environment. Nanostructures of ZnO of a variety of morphologies have been reported including nanowires, nanorods, tetrapods, nanobelts, nanoflowers, and nanoparticles.

ZnO is a piezoelectric semiconductor[76] with biocompatibility[77] and radiation hardness.[46,78] More importantly, although ZnO has a high melting point of >1900 °C which means it is highly stable, ZnO can be grown into different crystalline nanostructures on graphene in large scales and at low temperatures <100 °C in air, providing a direct pathway to practical applications.[79,80] The (0001) direction is the most favorable one for piezoelectricity in ZnO.[81–83] Wang and Song proposed the first ZnO nanowire-based piezoelectric nanogenerators,[23] which could convert nanoscale mechanical energy into electrical energy by means of piezoelectric effects. This pioneering work has prompted intensive research on various nanogenerators based on piezoelectric and triboelectric effects for mechanical energy harvesting and those based on thermoelectric and pyroelectric effects for thermal energy harvesting using ZnO and other materials.[84]

C. Compatibility of ZnO and graphene

Figures 2(a)–2(c) show the crystalline structure of graphene, a ZnO unit cell, and heterostructure nanohybrids of ZnO and graphene (ZnO/graphene) in which a heterostructure interface is formed between the two materials and will be shown to play a critical role in ZnO/graphene nanohybrid devices. It should be noted that both graphene and ZnO (in hexagonal wurtzite structure) have hexagonal lattice with lattice constants of 0.246 and 0.325 nm, respectively. This means heteroepitaxy of ZnO on graphene is possible with a careful control of the nucleation of the ZnO on graphene. Nevertheless, most reported ZnO/graphene heterostructure nanohybrids have a weak van der Waals (vdW) interface due to lack of control on the nucleation of ZnO on graphene that may be synthesized using mechanical exfoliation[85] or CVD.[86,87] Various ZnO deposition approaches have been reported including spin-coating,[88] drop casting,[26,89] and inkjet printing of pre-fabricated ZnO nanostructures,[34,90,91] and direct growth of ZnO on graphene using CVD,[92] hydrothermal growth,[11,12] sputtering,[29] atomic layer deposition (ALD),[93] spin-coating sol-gel precursors,[33,94,95] electrochemical deposition,[96] vapor transport,[45] etc. Considering most of these approaches can be carried out at either room temperature or low temperatures below 500 °C, the integrity of graphene could be preserved during the ZnO fabrication. Interestingly, graphene can remain intact when exposed to high temperatures up to 800°C for a

short time of 1–2 s in the so-called ultrafast thermal annealing to improve the nanojunctions between the ZnO nanoparticles (NPs) in the ZnO NP/graphene UV detectors.[95] Furthermore, these approaches are either ready or could be scaled up, for large-scale fabrication of ZnO. Therefore, ZnO/graphene nanohybrids can be fabricated in large scale at a low cost and are therefore promising for practical applications.

II. TRANSDUCTION OF SIGNALS TO GATING ON GRAPHENE IN ZNO/GRAPHENE HETEROSTRUCTURE NANOHYBRIDS

A. Gating effect on graphene

In ZnO/graphene nanohybrid devices, ZnO serves as a "sensitizer" to various external stimuli including light, mechanical deformation, gas or chemical molecules adsorption.[48] The unique physical properties of ZnO enable transduction of the stimuli to an electric field at the ZnO/graphene interface, which generates a gating effect on graphene channel and tunes the channel conductivity due to the unique ambipolar electric doping effect of graphene.[2,97] Figure 3(a) shows a graphene sheet resistance of n-type, p-type doped, in comparison with undoped, bilayer graphene field effect transistor (GFET) as a function of the applied back-gate voltage V_{BG} measured at room temperature in nitrogen atmosphere. The inset shows a schematic of the GFET.[98] The graphene sheet resistance of the undoped GFET is quite typical for a bilayer graphene GFET without a bandgap, exhibiting a sheet resistance of 8.7 kΩ at the Dirac point (charge neutrality point). As illustrated in Fig. 3(a), the Fermi energy for the intrinsic graphene has the minimal carrier concentration ~10^{12}/cm^2 and the Dirac point of maximum resistivity is located at $V_{BG} \sim 0$ (blue curve). When an external interface charge is introduced, graphene would be doped to either n-type (red) or p-type (green) as the Fermi energy is shifted upwards (above the Dirac point) or downwards (below the Dirac point). This means that the induced charges by external stimuli at the ZnO/graphene interface would cause a shift of the Fermi energy via charge doping and the polarity shift quantitatively would reflect the kind and amount of the interface charges generated by the stimuli. Figure 3(b) shows the V_{BG} dependence of graphene channel resistance measured on a GFET device, where the surface doping was detached by *in situ* annealing
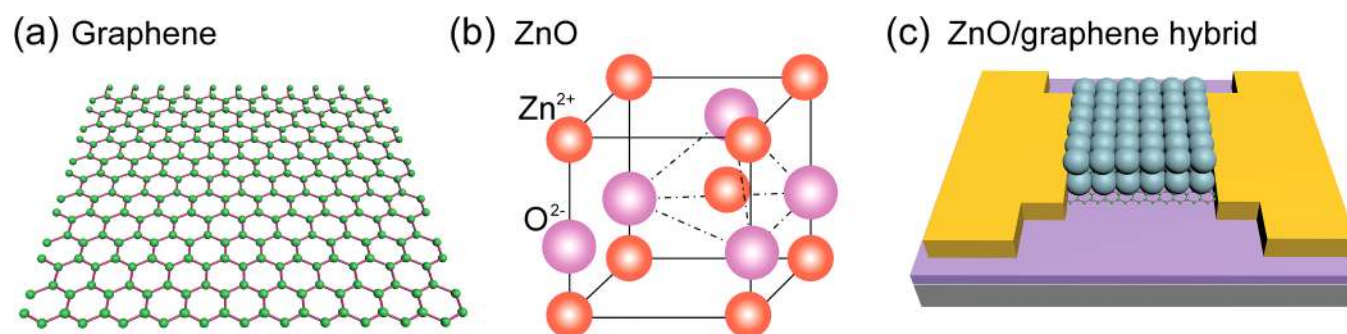

FIG. 2. Schematics of single-layer graphene sheet (a), ZnO crystal structure (b), and ZnO/graphene hybrid heterostructure (c).
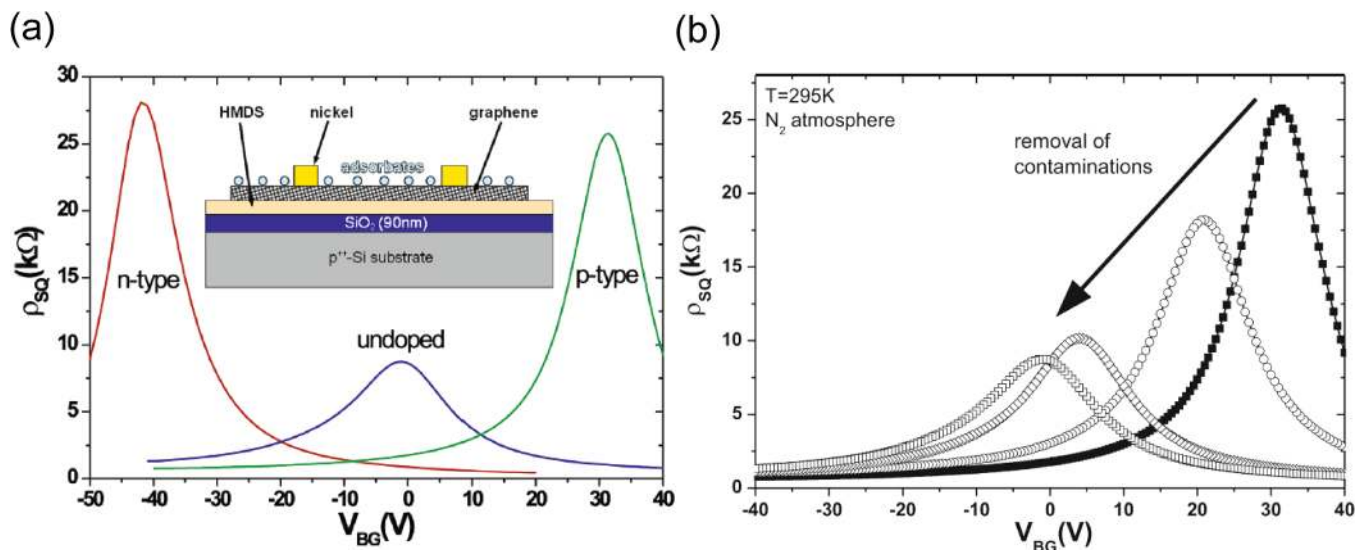
FIG. 3. (a) The resistance of a n-type, p-type, and an undoped bilayer graphene FET as a function of the applied back gate voltage measured at room temperature in nitrogen atmosphere. The inset shows a schematic of a graphene FET. The doping is realized by adsorbates. (b) Back gate dependent sheet resistance of a bilayer graphene device with atmospheric doping after fabrication (filled squares) and after annealing at 50 (circles), 100 (diamonds), and 150 °C (open squares) in nitrogen atmosphere. The data were collected at room temperature in nitrogen atmosphere. Reproduced with permission from Szafranek et al., Nano Lett. **11**, 2640 (2011).[98] Copyright 2011 American Chemical Society.

at 50, 100, and 150 °C in nitrogen atmosphere. In fact, the polar species trapped on the surface of graphene channel may cause doping in graphene, which could be removed using annealing and other methods developed.[9,98,99]

In the ZnO/graphene photodetectors, for example, excitons (electron–hole pairs) are generated upon UV light absorption by ZnO, followed by electrons transfer to graphene and holes trapped in ZnO, which leads to a built-in electric field at the ZnO/graphene interface.[9,33] Similarly, when (0001) crystalline ZnO nanowires are subjected to a mechanical deformation, the piezoelectric effect that is maximum along the (0001) axis would induce surface charges at the two ends of the ZnO nanowires. The surface charge at the ZnO nanowire/graphene interface would then generate the gating effect on graphene in the same way as in the ZnO/graphene photodetector case, which can modulate the graphene channel conductivity. Interestingly, when the mechanical deformation changes from tensile to compressive or vice versa, the ZnO nanowire/graphene interface build-in field changes polarity accordingly.[19,100] Chemical and gas sensors based on ZnO are based on the surface carrier depletion/accumulation effect, which can be maximum when the dimension of ZnO nanostructures is comparable to the Debye length (∼20 nm). Again, the adsorption of the analytes to the surface of ZnO nanostructures could cause charge separation and the appearance of the build-in field at the ZnO/graphene interface, resulting in the "responsivity" in a similar way to the ZnO/graphene photodetectors and strain sensors. The photoresponsivity (R*) is an important figure-of-merit for a photodetector and can be described as the photocurrent generated per unit power of absorbed incident light on the active area of a photodetector: $R^* = I_{ph}/P_{in}$.[9]

The I_{ph} characterizes the photocurrent equal to the illuminated current under illumination of incident power density (P_{in}) deduct dark current. Another important parameter used to represent the performance of a photodetector is the specific photodetectivity (D^*), which can be expressed as[10]

$$D^* = \frac{\sqrt{S \times \Delta f}}{NEP} \text{ (Jones),}$$

where S is the active area of a photodetector with a unit of cm^2, Δf (Hz) and NEP ($A/Hz^{1/2}$) are the bandwidth and noise equivalent power, respectively.

However, the performance of the ZnO/graphene nanohybrids devices depend sensitively on the ZnO surface states (defects, dangling bonds) and ZnO/graphene interface quality.[9,101,102] This is not difficult to understand since the nanohybrids rely on the ZnO/graphene interface gating effect. A defective interface with charge traps from adsorbed polar molecules to graphene, surface states of ZnO, chemical residues from processing can reduce or diminish charge transfer across ZnO/graphene interface and hence degrade the device performance. For example, charge traps can form on the ZnO QD surface and ZnO QD/graphene interface, resulting in low photoresponse and slow response speed.[48,97]

B. Fabrication of ZnO/graphene heterostructure nanohybrids

The most convenient way to construct ZnO/graphene heterostructure is growing ZnO directly on graphene. Among various

processes developed for ZnO growth, the solution-based one exhibits unique advantages for large-scale fabrication of ZnO/graphene heterostructure at low temperatures, low cost, and on flexible substrates. For example, highly crystalline ZnO NPs can be synthesized on graphene by spin-coating or inkjet printing of zinc acetate precursor, followed by annealing in air at temperatures <400 °C.[33] High-performance UV detection has been achieved by controlling the ZnO NP dimension on the order of the Debye length to allow electron depletion effect to be combined with graphene's high mobility for large photoconductive gain up to a few 1000 s. Liu *et al.* reported a seedless hydrothermal process by floating graphene face-down in solution to grow vertically aligned ZnO nanowire arrays (VANWs) on graphene.[12] Eliminating the ZnO seeding layer is important not only to simplify the ZnO/graphene heterostructure nanohybrids fabrication process but also to minimize damage to the sub-nanometer thickness graphene to maintain its high optical transmittance and conductivity. The seedless ZnO nanowires growth was found critical to obtain a low-defect ZnO-VANWs/Gr interface with minimal charge trapping for UV photodetection with faster photoresponse,[11] improved pressure/strain sensitivity of up to $3.15 \times 10^{-2}\,\mathrm{kPa^{-1}}$, and a dynamic response time of ∼0.10 s than in the case of ZnO-VANWs/graphene nanohybrids strain sensors.[19]

Beside the direct growth of ZnO on graphene, constructing ZnO/graphene hybrid heterostructure using pre-fabricated ZnO nanostructures is another commonly used method. Son *et al.* successfully employed spin-coating for deposition of ZnO QDs on graphene and obtained a nanohybrid UV photodetector.[103] At room temperature, the ratio of the photocurrent to the dark current is up to 1.1×10^4, and the rise and fall response times are approximately 2 and 1 s, respectively. Recently, Gong *et al.* reported a robust printing method to print ZnO QDs on the graphene channels of GFETs. The achieved ZnO QDs/GFET nanohybrid UV photodetectors exhibited an extraordinarily high photoresponsivity of $9.9 \times 10^8\,\mathrm{A/W}$ and a photoconductive gain of 3.6×10^9.[9] Compared to the direct growth of ZnO on graphene, the pre-fabrication ZnO nanostructures allow crystalline ZnO to be obtained in optimal growth window without concerns of graphene degradation, which is however at the cost of possible not optimal ZnO/graphene interface if the post-deposition of pre-fabricated ZnO is not fully controlled.

III. DEVELOPMENT OF ZNO/GRAPHENE NANOHYBRIDS OPTOELECTRONICS AND SENSORS

A. ZnO/graphene UV detectors

A photoconductive ZnO/graphene nanohybrid UV photodetector is geometrically characterized by two metal electrodes on the graphene layer, sometimes plus back gate tunability electrodes, which demonstrates a completely different operation mechanism from other photodetectors.[104] In these devices, ZnO of bandgap ∼3.3–3.4 eV serves as UV photosensitizers, and the excitons generated in ZnO could be dissociated by the build-in electric field at the ZnO/graphene interface, followed by charge transfer to graphene driven by the same built-in field. The photoresponse is a photo-gating effect on the conductance of the graphene channel measured from the source and drain electrodes. High photoconductive gain

up to 10^{10}–10^{12} can be achieved in the nanohybrid photodetectors.[9,105] The gain is defined as gain $= \tau_c/\tau_t$,[4,5,9,12,99] where τ_c is the exciton lifetime in ZnO, and τ_t is the carrier transit time in graphene channel which is defined as $\tau_t = l^2/\mu V_{bias}$, where l is the graphene channel length and V_{bias} is the source-drain bias voltage. Since τ_t is inversely proportional to the charge mobility μ in graphene,[106] the high gain in the ZnO/graphene nanohybrid UV detectors is primarily attributed to the high carrier mobility of graphene. In addition, ZnO nanostructures, such as QDs, NPs, and nanowires, may have a strong quantum confinement and hence high τ_c.[53,107] High gain can lead to high specific detectivity (D^*) as a major figure of the merit for a photodetector. On ZnO QD/graphene UV detectors, for example, high $D^* \sim 10^{13}$–10^{14} Jones has been demonstrated in (300–400 nm), respectively.[9,90,91,105] In these devices, the ZnO/graphene nanohybrid interface has been found to play a critical role in D^* and response speed. In the ZnO QD/graphene case, Gong *et al.* have confirmed that an atomic surface layer of ZnO QDs can block charge transfer across the QD/graphene interface and diminish D^*. Successful removal of this surface layer has led to $D^* \sim 10^{14}$ Jones as shown in Fig. 4.[9] Cook *et al.* compared ZnO nanowire/graphene UV detectors with ZnO nanowires grown on graphene in seeded and seedless processes. The ZnO seed layer was found defective and hence reduces the response speed.[11] In addition, flexible and sensitive ZnO nanowires/graphene nanohybrid UV photodetectors were also successfully assembled on polyethylene terephthalate (PET) substrates.[108] Remarkably, the impact of bending on the UV response was negligible after 10 000 bending cycles at a bending radius of 12 mm (or a strain of 0.5%).

B. ZnO/graphene strain sensors

High-performance strain sensors are desired for a large spectrum of emerging applications in wearable electronics,[109–111] robotics,[112] health care,[113] infrastructure monitoring.[114] Among others, piezoelectric/graphene nanohybrids are of particular interest to transduce a mechanical deformation from the piezoelectric component to the piezoelectric gating on graphene, taking the advantages of graphene's high mechanical strength,[115] flexibility, and high carrier mobility.[116] The piezoelectric nanohybrid strain sensors can be further divided into two main types: (1) piezoresistive[117,118] and (2) piezoelectric-gating[119,120] based on different sensing mechanisms. Piezoresistive strain sensors rely on resistance changes of piezoresistive materials under applied pressure/strain. The former has a simple device structure and low fabrication cost. However, the devices typically require a high power to operate[121] and hence a further improvement is necessary for them to be suitable for low-power or self-power applications.[122] In contrast to the piezoresistive devices that rely on the volume effect of the sensor, piezoelectric-gating devices based on the interface effect of the strain-induced piezoelectric surface charges may provide a promising scheme for strain sensors that could be operated at a low power.[123] In particular, (0001) ZnO VANWs/graphene nanohybrids that can be obtained by direct growth ZnO VANWs on graphene using a facile seedless hydrothermal process[11,12] combine the piezoelectric nanostructures and graphene allow a unique design of the piezoelectric-gating sensors.[80] Under mechanical strains, the induced piezoelectric effect in the ZnO nanowires transduces to a
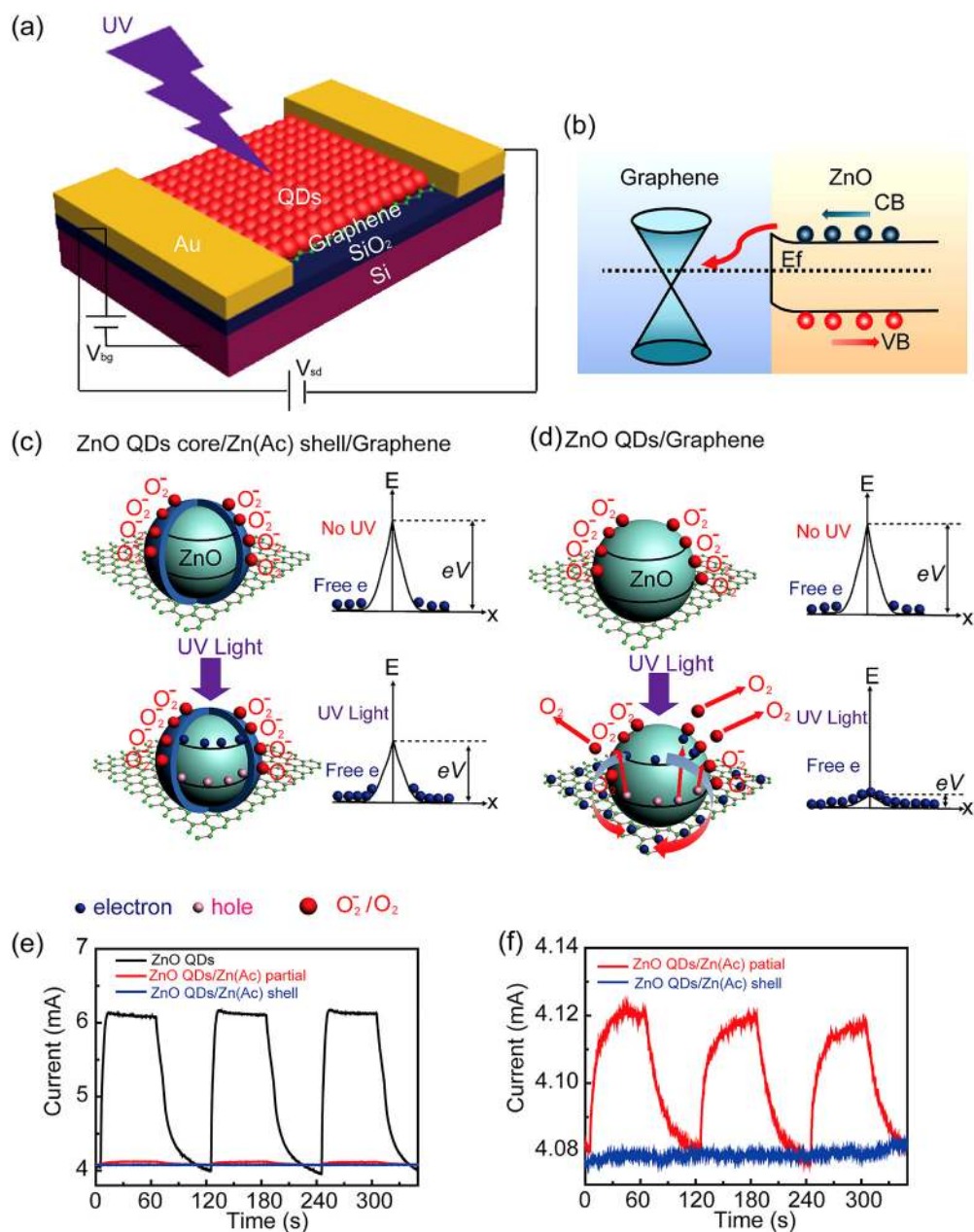
FIG. 4. (a) Schematic of the printed ZnO QDs/GFET hybrid UV photodetector. (b) Energy level diagram of ZnO QDs/GFET heterojunctions and charge transfer process under UV illumination. The band energy diagram (c) with and (d) without Zn(Ac) charge transfer blocking shell in the dark and under illumination of UV light, associated with oxygen adsorption/desorption and charge transfer process. (e) The dynamic photoresponse of ZnO QDs/graphene photodetectors with and without Zn(Ac) blocking shell. (f) Zoomed-in view of the dynamic photoresponse on ZnO QDs with partial and full Zn(Ac) blocking shell. Reproduced with permission from Gong *et al.*, ACS Nano **11**, 4114 (2017). Copyright 2017 American Chemical Society.

piezoelectric gating effect at the ZnO/graphene interface, resulting in a modulation of the conductivity of the graphene channel through electrostatic doping. The vertical alignment of the (0001) oriented ZnO nanowires on graphene is ideal to achieving high

strain sensitivity and a low-defect ZnO/graphene interface obtained in the seedless hydrothermal process is key to realizing high sensitivity and fast response. Indeed, high sensitivity up to $3.15 \times 10^{-2}\,\mathrm{kPa}^{-1}$ was obtained on the ZnO nanowire/graphene
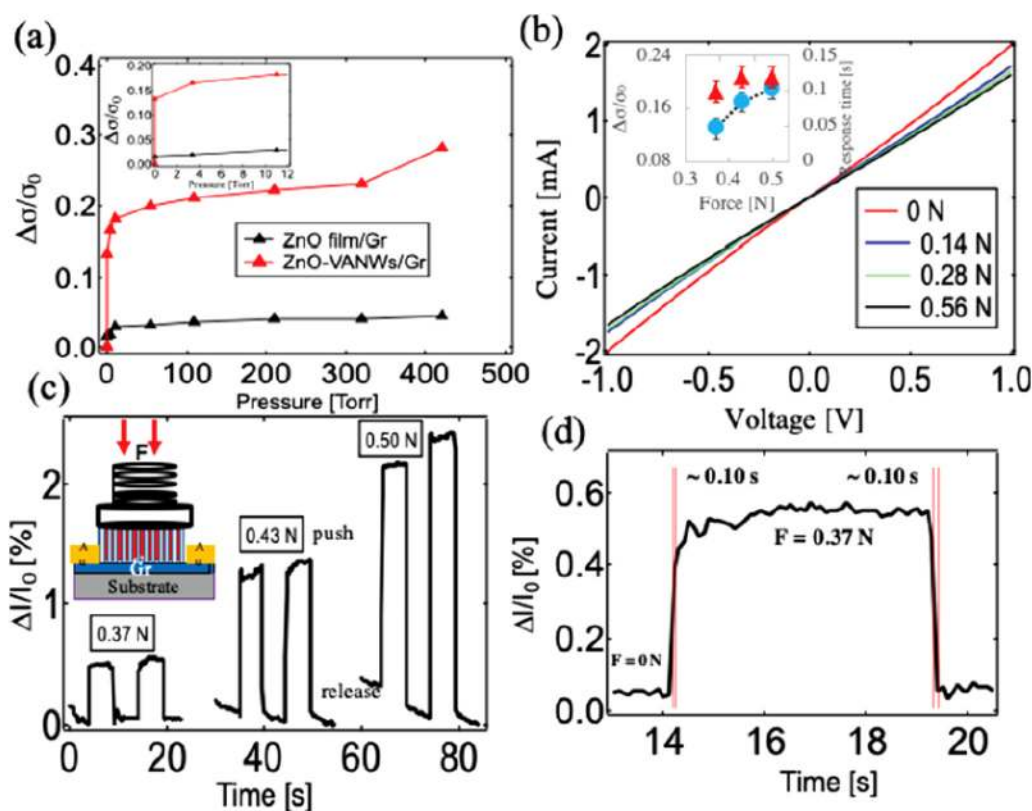
FIG. 5. (a) Characterization of the ZnO-VANWs/graphene and ZnO film/graphene strain sensors. $\Delta\sigma/\sigma_0$ as a function of gas pressure measured on ZnO-VANWs/graphene (red) and ZnO film/graphene (black) devices. (b) *I–V* curves collected on the ZnO-VANWs/graphene devices at different forces applied using the spring apparatus. The inset shows the sensitivity and response time as a function of forces. (c) Dynamic strain response at different forces of 0.37, 0.43, and 0.50 N. The inset shows schematic of the spring apparatus. (d) Zoomed-in views of the dynamic strain response with the corresponding response times illustrated. Reproduced with permission from Panth *et al.*, ACS Appl. Nano Mater. **3**, 6711(2020). Copyright 2020 American Chemical Society.

strain sensors at lower pressure of 1.1×10^{-6}–11 Torr, together with a fast response time of ∼0.10 s as shown in Fig. 5(d). On flexible PET substrates, the sensors show high responsivity to mechanical bending.[100] Under the mechanical bending curvatures of 0.18, 0.23, 0.37, and 0.45 cm^{-1}, respectively, high sensitivity of the gauge factors up to ∼248 and response times of 0.20 s/0.20 s (rise/fall) were achieved. Moreover, the response changes polarity when the directions of bending alter between up and down, corresponding to the polarity change of the space charge on the ZnO nanowire/graphene interface as a consequence of the compressive and tensile strains along the ZnO nanowires.

C. ZnO/graphene chemical and gas sensors

The release of harmful and toxic chemicals and gases extremely endangers social and environmental safety and human health. Sensitive detection of these chemicals and gases is needed to protect the health and safety of our society. ZnO based gas sensors have been widely developed ascribing to their high selectivity, low manufacturing cost, low detection limit, and reliable

performance.[124] In addition, graphene exhibits extraordinary electrical and structural properties rendering it attractive for flexible graphene-based gas sensor applications. It should be realized that graphene alone could be used for gas sensing due to the variation in its electrical conductivity stimulated by the gas molecules adsorption due to the facile manipulation of the Fermi level by charge gating effect on graphene.[125,126] Nevertheless, owing to its chemical inertness, the gas molecules are preferentially targeted to the defects or structurally unstable sites on graphene, such as unavoidably occurring oxygen related functional groups and grain boundaries. This results in insufficient power of the cyclic and reliable gas response due to the weak gas desorption. Different from the ZnO or graphene only cases, the ZnO/graphene heterostructure nanohybrids can exhibit much improved performance in gas sensing due to increased sensor surface area of ZnO nanostructures and graphene and the high charge carrier mobility for improved response time. Muchtar *et al.* reported ZnO/graphene nanohybrid carbon monoxide gas sensors fabricated using a reflow method.[127] It was found that the ZnO/graphene nanohybrid structure exhibited the potential to improve the sensitivity under low temperature

conditions as compared to the ZnO only counterpart. Specifically, these ZnO/graphene sensors demonstrated ~36% response at 125 °C, while the ZnO only counterpart did not even show measurable response at the same operating temperature. In addition, Bae *et al.* reported a new approach to design dual-channel NO₂ gas sensors on the basis of a role-allocated ZnO/graphene heterostructure, formed by the complementary hybridization of graphene and a ZnO thin film as shown in Fig. 6(a).[128] This design enables cyclic and reproducible gas response as well as high gas responsivity. The ZnO top layer acted as a gas adsorption layer and graphene bottom layer served as the signal conducting layer. Remarkably, a reliable and abrupt gas response under periodic NO₂ gas injection was obtained, which is ~30 times higher than that of the graphene-only counterparts. In general, the ZnO/graphene heterostructure nanohybrids provide a platform for design of various gas and chemical sensors with high sensitivity and reproducibility.

D. Other ZnO/graphene nanohybrids devices

Besides UV photodetectors, strain sensors, and chemical/gas sensors, ZnO/graphene heterostructure has also been implemented in many other applications including solar cells, LEDs, waveguides, and high-performance UV lasers.[21,88,129,130] For example, the UV lasing based on ZnO materials has been reported in various micro/nanostructures over whispering-gallery mode (WGM)[131] and random Fabry–Pérot (FP)[132,133] resonant approaches. However, the diffraction limit and huge cavity losses made it difficult to fabricate micro/nanostructure lasers with high efficiency.[134] Although surface plasmon (SP)-mediated photoluminescence (PL) enhancement has been observed at metal–ZnO nanostructure interfaces, it was difficult to design flexible and novel photonic devices due to the required rigid substrates and large Ohmic losses.[135] Fortunately, graphene has recently shown a very high quantum efficiency for strong plasmons and light-matter interaction, which means that the ZnO/graphene heterostructure could provide a potential candidate for UV lasing with improved performance.[136] Li *et al.* reported optical field confinement and PL enhancement induced by graphene's SP both experimentally and theoretically on a ZnO/graphene heterostructure, which served as a whispering-gallery mode (WGM) for lasing resonance.[137] Indeed, improved WGM lasing performance including stronger lasing intensity, lower threshold, and higher quality factor (Q) has been realized. The same group also reported (Fabry–Pérot) F-P lasing performance improvement through the coupling between graphene's SP modes and
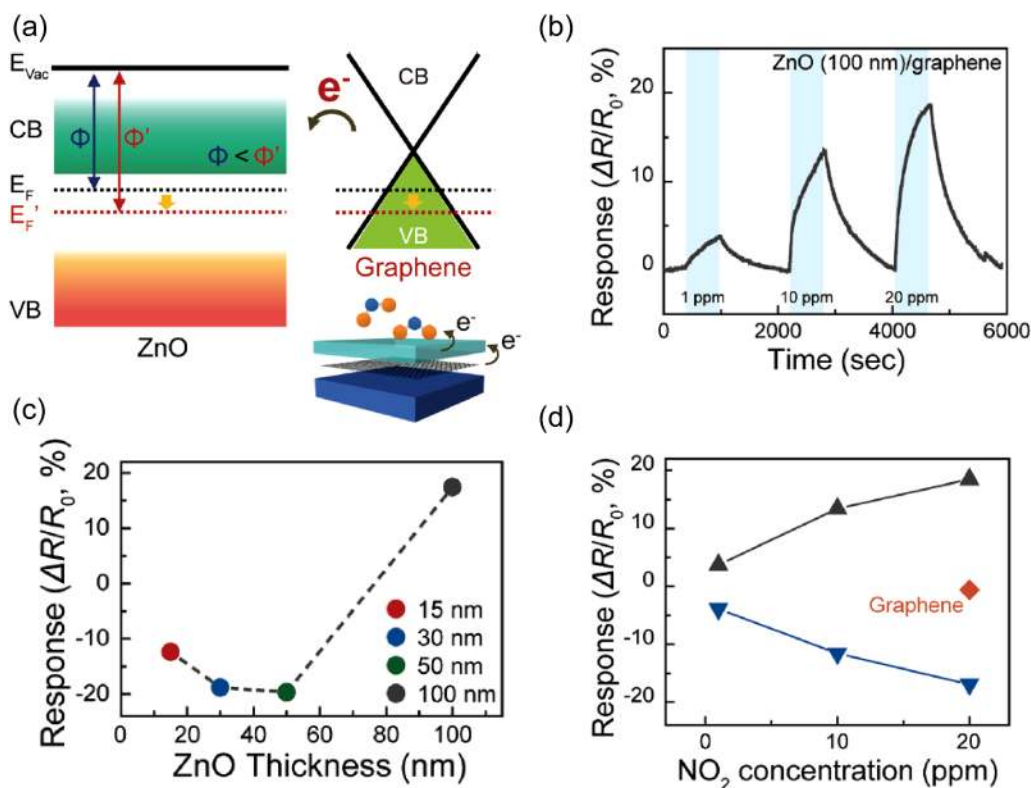

FIG. 6. (a) The schematic of the electronic band structure of graphene and ZnO showing Fermi level shift by the charge compensation after introducing NO₂ gas. (b) Cyclic gas response curves for various concentrations (1, 10, and 20 ppm) of NO₂ measured at 250 °C. (c) Plots of extracted NO₂ gas response for the thickness-controlled ZnO /graphene-based gas sensors. (d) Plots of extracted NO₂ gas response for ZnO (30, 100 nm)/graphene as a function of the concentration of NO₂. Reproduced with permission from Bae *et al.*, ACS Appl. Mater. Interfaces **11**, 16830 (2019). Copyright 2019 American Chemical Society.
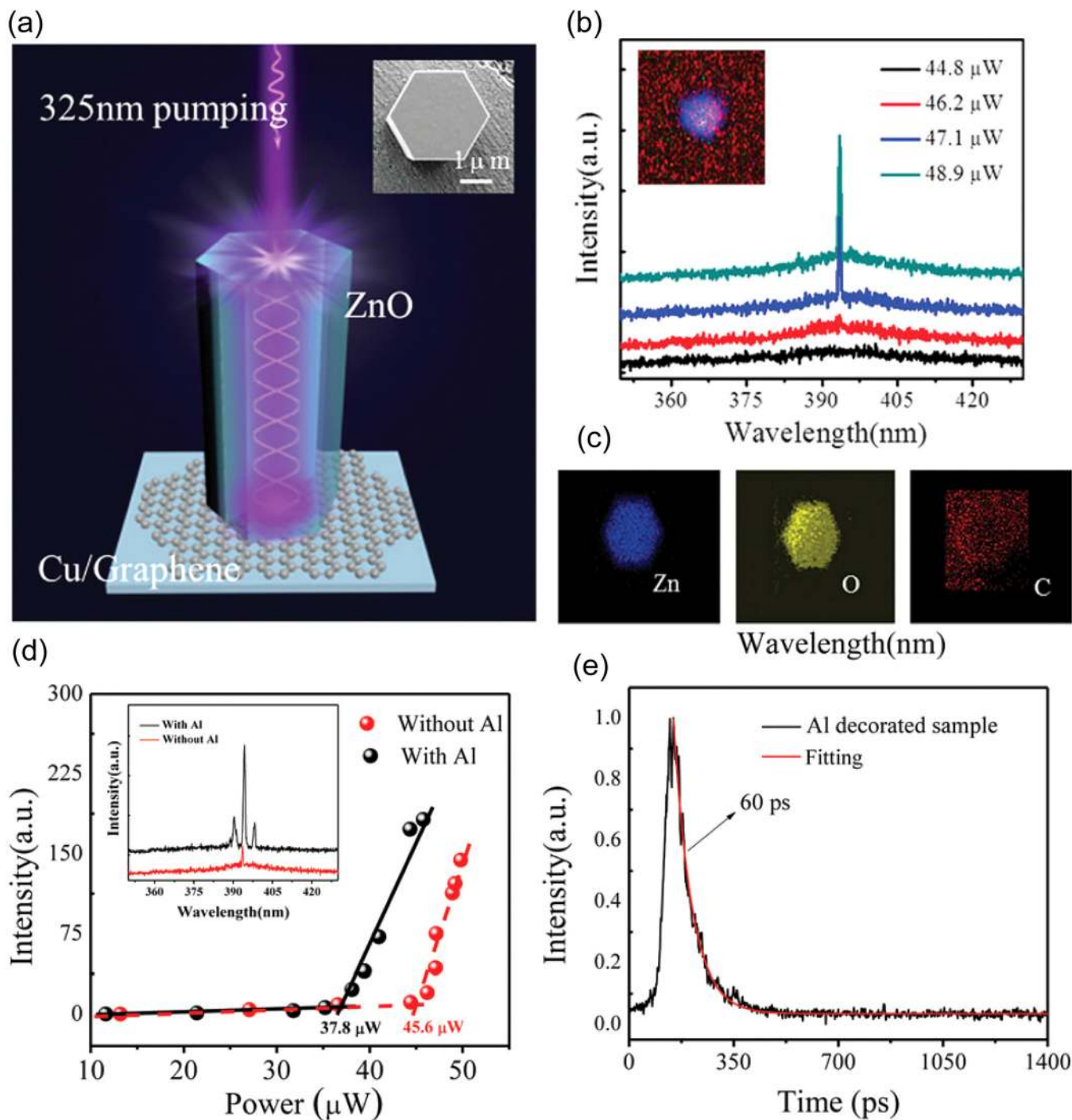
FIG. 7. (a) Schematic of a ZnO microlaser optically excited by a 325 nm fermi second laser. The inset shows an SEM image of an individual ZnO microrod. [(b) and (c)] Lasing spectra of an individual ZnO microrod at different excitation powers and EDX mapping of ZnO on graphene. (d) Lasing intensity vs pumping power with and without Al decoration, the inset shows the lasing spectra under the same excitation power density. (e) Time resolved spectral response tested on Al decorated ZnO/graphene, fitted by the single-exponential function. Reproduced with permission from Qin et al., J. Mater. Chem. C **6**, 3240 (2018). Copyright 2018 The Royal Society of Chemistry.

conventional optical microcavity modes of ZnO, which includes the improved lasing quality, lowered lasing threshold, and remarkably enhanced lasing intensity.[138]

Recently, high-performance single-mode lasing has received much attention ascribing to lower lasing threshold, high Q factor, and narrow spectral linewidth due to the total internal wall refection of the microcavity.[139] Qin et al. reported a high Q single-mode lasing on ZnO/graphene heterostructure (as shown in Fig. 7).[21] Compared with the ZnO nanorods, this ZnO/graphene heterostructure has better structural and higher light emission intensity. The individual ZnO nanorod grown on graphene was chosen as a lasing cavity to realize single mode lasing with a central wavelength of 393.2 nm as shown in Fig. 7(b). The obtained Q factor is 936, which is greater than that achieved in ZnO-only microstructures. After decoration of Al, the exciton recombination rate was increased, realizing intensity enhanced multimode lasing as shown in Fig. 7(d).

IV. SUMMARY AND FUTURE REMARKS

In summary, ZnO/graphene heterostructure nanohybrids combine the unique physical properties of ZnO and graphene, providing a unique scheme for exploration of functional devices ranging from photodetectors, strain sensors, touch screens, chemical and gas sensors, self-powered devices, etc. These nanohybrids differ from ZnO only counterpart devices in the sense that charge transport occurs primarily in graphene, taking advantage of its extraordinary high charge mobility, which is the key to high device performance that would otherwise impossible. In the ZnO QDs/graphene nanohybrid UV detectors, for example, the strong quantum confinement in both ZnO QDs and graphene has shown to lead to a high photoconductive gain of $\sim 10^{10}$ or higher, and hence high $D^* \sim 10^{14}$ Jones as demonstrated already. In addition, the availability of large-area monolayer graphene and the feasibility of device fabrication on graphene using standard microfabrication are critical to practical applications. These, in combination of the compatibility of growth condition of ZnO to graphene enable a layer-by-layer growth of the ZnO, particularly functional crystalline ZnO nanostructures with controlled morphology and orientation on graphene, which is important not only to controlling the ZnO/graphene interface that impacts the ZnO/graphene nanohybrid device performance, but also to scaling up for commercial applications of ZnO/graphene nanohybrid devices on both rigid and flexible substrates. Finally, a distinctive advantage of ZnO/graphene nanohybrids is that the entire sample can be flexible when made on flexible substrates. Considering the wide bandgap and ferroelectric (as well as piezoelectric) properties of ZnO, ZnO/graphene nanohybrids will certainly prompt new research studies in exploration of combination of such properties of ZnO with ambipolar gating effect of graphene in flexible and self-powered electronic, photonic, optoelectronic, and electrochemical applications of ZnO/graphene nanohybrids. Therefore, ZnO/graphene heterostructure nanohybrids have unique advantages over their ZnO-only nanostructure counterparts in terms of physical properties enabled by the strong quantum confinement in both ZnO nanostructures and graphene, the ZnO/graphene interface build-in electric field to facilitate charge transfer which is critically important to applications such as

electronic, optoelectronic and electrochemical, and the charge transport in graphene of superior carrier mobility. However, the ZnO/graphene interface also introduces a major "disadvantage" or more accurately challenge in R&D of ZnO/graphene heterostructure nanohybrids. One of the critical issues is in controlling the ZnO/graphene interface to eliminate defects that can reduce the responsivity and response speed of the ZnO/graphene nanohybrid devices. Another issue is in controlling the uniformity of the ZnO/graphene at multiple scales. This requires the development of new approaches to achieve an atomic control on the surfaces and interfaces and will be a focus of future research on ZnO/graphene nanohybrids.

DATA AVAILABILITY

The data that support the findings of this study are available from the corresponding author upon reasonable request.

REFERENCES

[1]K. S. Novoselov, A. K. Geim, S. V. Morozov, D. Jiang, Y. Zhang, S. V. Dubonos, I. V. Grigorieva, and A. A. Firsov, "Electric field effect in atomically thin carbon films," Science 306, 666 (2004).
[2]A. K. Geim and K. S. Novoselov, "The rise of graphene," Nat. Mater. 6, 183 (2007).
[3]X. S. Li, W. W. Cai, J. H. An, S. Kim, J. Nah, D. X. Yang, R. Piner, A. Velamakanni, I. Jung, E. Tutuc, S. K. Banerjee, L. Colombo, and R. S. Ruoff, "Large-area synthesis of high-quality and uniform graphene films on copper foils," Science 324, 1312 (2009).
[4]G. Konstantatos, M. Badioli, L. Gaudreau, J. Osmond, M. Bernechea, F. P. G. de Arquer, F. Gatti, and F. H. L. Koppens, "Hybrid graphene-quantum dot photo-transistors with ultrahigh gain," Nat. Nanotechnol. 7, 363 (2012).
[5]A. K. Geim and I. V. Grigorieva, "Van der Waals heterostructures," Nature 499, 419 (2013).
[6]J. Z. Wu, in Transparent Conductive Materials: Materials, Synthesis, Characterization, Applications, edited by D. Levy and E. Castellon (Wiley-VCH, Weinheim, 2019), Vol. 1, p. 165.
[7]M. Gong, D. Ewing, M. Casper, A. Stramel, A. Elliot, and J. Z. Wu, "Controllable synthesis of monodispersed Fe$_{1-x}$S$_2$ nanocrystals for high-performance optoelectronic devices," ACS Appl. Mater. Interfaces 11, 19286 (2019).
[8]M. Gong, R. Sakidja, Q. Liu, R. Goul, D. Ewing, M. Casper, A. Stramel, A. Elliot, and J. Z. Wu, "Broadband photodetectors: Broadband photodetectors enabled by localized surface plasmonic resonance in doped iron pyrite nanocrystals," Adv. Opt. Mater. 6, 1870033 (2018).
[9]M. Gong, Q. Liu, B. Cook, B. Kattel, T. Wang, W. L. Chan, D. Ewing, M. Casper, A. Stramel, and J. Z. Wu, "All-printable ZnO quantum dots/graphene van der Waals heterostructures for ultrasensitive detection of ultraviolet light," ACS Nano 11, 4114 (2017).
[10]M. Gong, R. Sakidja, R. Goul, D. Ewing, M. Casper, A. Stramel, A. Elliot, and J. Z. Wu, "High-performance all-inorganic CsPbCl$_3$ perovskite nanocrystal photodetectors with superior stability," ACS Nano 13, 1772 (2019).
[11]B. Cook, Q. F. Liu, J. W. Liu, M. G. Gong, D. Ewing, M. Casper, A. Stramel, and J. D. Wu, "Facile zinc oxide nanowire growth on graphene via a hydrothermal floating method: Towards debye length radius nanowires for ultraviolet photodetection," J. Mater. Chem. C 5, 10087 (2017).

[12]J. Liu, R. Lu, G. Xu, J. Wu, P. Thapa, and D. Moore, "Development of a seedless floating growth process in solution for synthesis of crystalline ZnO micro/nanowire arrays on graphene: Towards high-performance nanohybrid ultraviolet photodetectors," Adv. Funct. Mater. **23**, 4941 (2013).

[13]K. Roy, M. Padmanabhan, S. Goswami, T. P. Sai, G. Ramalingam, S. Raghavan, and A. Ghosh, "Graphene–MoS$_2$ hybrid structures for multifunctional photoresponsive memory devices," Nat. Nanotechnol. **8**, 826 (2013).

[14]F. Xia, H. Wang, D. Xiao, M. Dubey, and A. Ramasubramaniam, "Two-dimensional material nanophotonics," Nat. Photonics **8**, 899 (2014).

[15]S. Kim, J. Nah, I. Jo, D. Shahrjerdi, L. Colombo, Z. Yao, E. Tutuc, and S. K. Banerjee, "Realization of a high mobility dual-gated graphene field-effect transistor with Al$_2$O$_3$ dielectric," Appl. Phys. Lett. **94**, 062107 (2009).

[16]B. Zhan, C. Li, J. Yang, G. Jenkins, W. Huang, and X. Dong, "Graphene field-effect transistor and its application for electronic sensing," Small **10**, 4042 (2014).

[17]E. Fortunato, P. Barquinha, and R. Martins, "Oxide semiconductor thin-film transistors: A review of recent advances," Adv. Mater. **24**, 2945 (2012).

[18]M. Gong, P. Adhikari, Y. Gong, T. Wang, Q. Liu, B. Kattel, W.-Y. Ching, W.-L. Chan, and J. Z. Wu, "Polarity-controlled attachment of cytochrome c for high-performance cytochrome c/graphene van der Waals heterojunction photodetectors," Adv. Funct. Mater. **28**, 1704797 (2018).

[19]M. Panth, B. Cook, Y. Zhang, D. Ewing, A. Tramble, A. Wilson, and J. Wu, "High-performance strain sensors based on vertically aligned piezoelectric zinc oxide nanowire array/graphene nanohybrids," ACS Appl. Nano Mater. **3**, 6711 (2020).

[20]S. Sun, L. Guo, X. Chang, Y. Liu, S. Niu, Y. Lei, T. Liu, and X. Hu, "A wearable strain sensor based on the ZnO/graphene nanoplatelets nanocomposite with large linear working range," J. Mater. Sci. **54**, 7048 (2019).

[21]F. F. Qin, C. X. Xu, Q. X. Zhu, J. F. Lu, F. Chen, D. T. You, Z. Zhu, and A. G. Manohari, "Optical performance improvement in hydrothermal ZnO/graphene structures for ultraviolet lasing," J. Mater. Chem. C **6**, 3240 (2018).

[22]J. Rodrigues, J. Zanoni, G. Gaspar, A. J. S. Fernandes, A. F. Carvalho, N. F. Santos, T. Monteiro, and F. M. Costa, "ZnO decorated laser-induced graphene produced by direct laser scribing," Nanoscale Adv. **1**, 3252 (2019).

[23]Z. L. Wang and J. Song, "Piezoelectric nanogenerators based on zinc oxide nanowire arrays," Science **312**, 242 (2006).

[24]J. Briscoe and S. Dunn, "Piezoelectric nanogenerators—A review of nanostructured piezoelectric energy harvesters," Nano Energy **14**, 15 (2015).

[25]W. Guo, S. Xu, Z. Wu, N. Wang, M. M. Loy, and S. Du, "Oxygen-assisted charge transfer between ZnO quantum dots and graphene," Small **9**, 3031 (2013).

[26]M. Padmanabhan, R. Meyen, and K. Houghton, "Facile fabrication of ZnO–graphite composite thin films for ultraviolet photodetection," Mater. Res. Express **5**, 095606 (2018).

[27]S. Kim, Y. J. Choi, Y. Choi, M. S. Kang, and J. H. Cho, "Large-area Schottky barrier transistors based on vertically stacked graphene-metal oxide heterostructures," Adv. Funct. Mater. **27**, 1700651 (2017).

[28]A. Monreal-Bernal and J. Vilatela, "Large-area Schottky junctions between zno and carbon nanotube fibres," ChemPlusChem **83**, 285 (2018).

[29]B. Nie, J. G. Hu, L. B. Luo, C. Xie, L. H. Zeng, P. Lv, F. Z. Li, J. S. Jie, M. Feng, C. Y. Wu, Y. Q. Yu, and S. H. Yu, "Monolayer graphene film on ZnO nanorod array for high-performance Schottky junction ultraviolet photodetectors," Small **9**, 2872 (2013).

[30]R. Yatskiv and J. Grym, "Temperature-dependent properties of semimetal graphite-ZnO Schottky diodes," Appl. Phys. Lett. **101**, 162106 (2012).

[31]Z. Zhu, S. Wang, Y. Zhu, X. Liu, Y. Zou, Y. Gu, D. Ju, and H. Zeng, "Fiber-shaped ZnO/graphene Schottky photodetector with strain effect," Adv. Mater. Interfaces **5**, 1800136 (2018).

[32]Y. Ning, Z. Zhang, F. Teng, and X. Fang, "Novel transparent and self-powered UV photodetector based on crossed ZnO nanofiber array homojunction," Small **14**, e1703754 (2018).

[33]Q. F. Liu, M. G. Gong, B. Cook, D. Ewing, M. Casper, A. Stramel, and J. Wu, "Transfer-free and printable graphene/ZnO-nanoparticle nanohybrid photodetectors with high performance," J. Mater. Chem. C **5**, 6427 (2017).

[34]B. Cook, Q. Liu, M. Gong, D. Ewing, M. Casper, A. Stramel, and J. Wu, "Quantum dots-facilitated printing of ZnO nanostructure photodetectors with improved performance," ACS Appl. Mater. Interfaces **9**, 23189 (2017).

[35]H. Y. Lee, Y. C. Heish, and C. T. Lee, "High sensitivity detection of nitrogen oxide gas at room temperature using zinc oxide-reduced graphene oxide sensing membrane," J. Alloys Compd. **773**, 950 (2019).

[36]R. Yatskiv, J. Grym, P. Gladkov, O. Cernohorsky, J. Vanis, J. Maixner, and J. H. Dickerson, "Room temperature hydrogen sensing with the graphite/ZnO nanorod junctions decorated with Pt nanoparticles," Solid State Electron. **116**, 124 (2016).

[37]H. Tian, H. Fan, M. Li, and L. Ma, "Zeolitic imidazolate framework coated ZnO nanorods as molecular sieving to improve selectivity of formaldehyde gas sensor," ACS Sens. **1**, 243 (2016).

[38]H. Tian, H. Fan, J. Ma, Z. Liu, L. Ma, S. Lei, J. Fang, and C. Long, "Pt-decorated zinc oxide nanorod arrays with graphitic carbon nitride nanosheets for highly efficient dual-functional gas sensing," J. Hazard. Mater. **341**, 102 (2018).

[39]L. Ma, H. Fan, H. Tian, J. Fang, and X. Qian, "The n-ZnO/n-In$_2$O$_3$ heterojunction formed by a surface-modification and their potential barrier-control in methanal gas sensing," Sens. Actuators B: Chem. **222**, 508 (2016).

[40]Z. Chen, Z. Wang, X. Li, Y. Lin, N. Luo, M. Long, N. Zhao, and J. B. Xu, "Flexible piezoelectric-induced pressure sensors for static measurements based on nanowires/graphene heterostructures," ACS Nano **11**, 4507 (2017).

[41]S. H. Shin, D. H. Park, J. Y. Jung, M. H. Lee, and J. Nah, "Ferroelectric zinc oxide nanowire embedded flexible sensor for motion and temperature sensing," ACS Appl. Mater. Interfaces **9**, 9233 (2017).

[42]N. Gao and X. Fang, "Synthesis and development of graphene-inorganic semiconductor nanocomposites," Chem. Rev. **115**, 8294 (2015).

[43]A. H. Castro Neto, F. Guinea, N. M. R. Peres, K. S. Novoselov, and A. K. Geim, "The electronic properties of graphene," Rev. Mod. Phys. **81**, 109 (2009).

[44]F.-X. Liang, Y. Gao, C. Xie, X.-W. Tong, Z.-J. Li, and L.-B. Luo, "Recent advances in the fabrication of graphene–ZnO heterojunctions for optoelectronic device applications," J. Mater. Chem. C **6**, 3815 (2018).

[45]E. A. Azhar, J. Vanjaria, S. Ahn, T. Fou, S. K. Dey, T. Salagaj, N. Sbrockey, G. S. Tompa, and H. Yu, "Vapor-transport synthesis and annealing study of Zn$_x$Mg$_{1-x}$O nanowire arrays for selective, solar-blind UV-c detection," ACS Omega **3**, 4899 (2018).

[46]A. Janotti and C. G. Van de Walle, "Fundamentals of zinc oxide as a semiconductor," Rep. Prog. Phys. **72**, 126501 (2009).

[47]M. Gong, M. Alamri, D. Ewing, S. M. Sadeghi, and J. Z. Wu, "Localized surface plasmon resonance enhanced light absorption in AuCu/CsPbCl$_3$ core/shell nanocrystals," Adv. Mater. **32**, 2002163 (2020).

[48]J. Z. Wu and M. Gong, "Nanohybrid photodetectors," Adv. Photon. Res. **2**, 2100015 (2021).

[49]K. S. Novoselov, A. K. Geim, S. V. Morozov, D. Jiang, M. I. Katsnelson, I. V. Grigorieva, S. V. Dubonos, and A. A. Firsov, "Two-dimensional gas of massless dirac fermions in graphene," Nature **438**, 197 (2005).

[50]S. De and J and N. Coleman, "Are there fundamental limitations on the sheet resistance and transmittance of thin graphene films?," ACS Nano **4**, 2713 (2010).

[51]S. Stankovich, D. A. Dikin, G. H. B. Dommett, K. M. Kohlhaas, E. J. Zimney, E. A. Stach, R. D. Piner, S. T. Nguyen, and R. S. Ruoff, "Graphene-based composite materials," Nature **442**, 282 (2006).

[52]R. R. Nair, P. Blake, A. N. Grigorenko, K. S. Novoselov, T. J. Booth, T. Stauber, N. M. R. Peres, and A. K. Geim, "Fine structure constant defines visual transparency of graphene," Science **320**, 1308 (2008).

[53]J. H. Chen, C. Jang, S. D. Xiao, M. Ishigami, and M. S. Fuhrer, "Intrinsic and extrinsic performance limits of graphene devices on SiO$_2$," Nat. Nanotechnol. **3**, 206 (2008).

[54]F. Bonaccorso, Z. Sun, T. Hasan, and A. C. Ferrari, "Graphene photonics and optoelectronics," Nat. Photonics **4**, 611 (2010).

[55]S. Bae, H. Kim, Y. Lee, X. Xu, J. S. Park, Y. Zheng, J. Balakrishnan, T. Lei, H. R. Kim, Y. I. Song, Y. J. Kim, K. S. Kim, B. Özyilmaz, J. H. Ahn, B. H. Hong,

and S. Iijima, "Roll-to-roll production of 30-inch graphene films for transparent electrodes," Nat. Nanotechnol. **5**, 574 (2010).

[56] A. B. Sproul and M. A. Green, "Intrinsic carrier concentration and minority-carrier mobility of silicon from 77 to 300 k," J. Appl. Phys. **73**, 1214 (1993).

[57] J. M. Luther, P. K. Jain, T. Ewers, and A. P. Alivisatos, "Localized surface plasmon resonances arising from free carriers in doped quantum dots," Nat. Mater. **10**, 361 (2011).

[58] R. G. Gordon, "Criteria for choosing transparent conductors," MRS Bull. **25**, 52 (2000).

[59] J. K. Wassei and R. B. Kaner, "Graphene, a promising transparent conductor," Mater. Today **13**, 52 (2010).

[60] M. Orlita and M. Potemski, "Dirac electronic states in graphene systems: Optical spectroscopy studies," Semicond. Sci. Technol. **25**, 063001 (2010).

[61] V. G. Kravets, A. N. Grigorenko, R. R. Nair, P. Blake, S. Anissimova, K. S. Novoselov, and A. K. Geim, "Spectroscopic ellipsometry of graphene and an exciton-shifted van hove peak in absorption," Phys. Rev. B **81**, 155413 (2010).

[62] F. J. Nelson, V. K. Kamineni, T. Zhang, E. S. Comfort, J. U. Lee, and A. C. Diebold, "Optical properties of large-area polycrystalline chemical vapor deposited graphene by spectroscopic ellipsometry," Appl. Phys. Lett. **97**, 253110 (2010).

[63] K. Wang, J. J. Chen, Z. M. Zeng, J. Tarr, W. L. Zhou, Y. Zhang, Y. F. Yan, C. S. Jiang, J. Pern, and A. Mascarenhas, "Synthesis and photovoltaic effect of vertically aligned ZnO/ZnS core/shell nanowire arrays," Appl. Phys. Lett. **96**, 123105 (2010).

[64] J. W. Weber, V. E. Calado, and M. C. M. van de Sanden, "Optical constants of graphene measured by spectroscopic ellipsometry," Appl. Phys. Lett. **97**, 091904 (2010).

[65] M. Gong, X. Xu, Z. Yang, Y. Liu, H. Lv, and L. Lv, "A reticulate superhydrophobic self-assembly structure prepared by ZnO nanowires," Nanotechnology **20**, 165602 (2009).

[66] Z. L. Wang, "Zno nanowire and nanobelt platform for nanotechnology," Mater. Sci. Eng.: R: Rep. **64**, 33 (2009).

[67] Z. L. Wang, "Nanostructures of zinc oxide," Mater. Today **7**, 26 (2004).

[68] Z. L. Wang, "Zinc oxide nanostructures: Growth, properties and applications," J. Phys.: Condens. Matter **16**, R829 (2004).

[69] M. Gong, Z. Yang, X. Xu, D. Jasion, S. Mou, H. Zhang, Y. Long, and S. Ren, "Superhydrophobicity of hierarchical ZnO nanowire coatings," J. Mater. Chem. A **2**, 6180 (2014).

[70] M. Gong, X. Xu, Z. Cao, Y. Liu, and H. Zhu, "Two-step growth of superhydrophobic ZnO nanorod array films," Acta Phys. Sin. **58**, 1885 (2009).

[71] A. Ashrafi and C. Jagadish, "Review of zincblende ZnO: Stability of metastable ZnO phases," J. Appl. Phys. **102**, 071101 (2007).

[72] C. Pan, J. Zhai, and Z. L. Wang, "Piezotronics and piezo-phototronics of third generation semiconductor nanowires," Chem. Rev. **119**, 9303 (2019).

[73] Q. Zheng, B. Shi, Z. Li, and Z. L. Wang, "Recent progress on piezoelectric and triboelectric energy harvesters in biomedical systems," Adv. Sci. **4**, 1700029 (2017).

[74] W. Y. Nie, H. H. Tsai, R. Asadpour, J. C. Blancon, A. J. Neukirch, G. Gupta, J. J. Crochet, M. Chhowalla, S. Tretiak, M. A. Alam, H. L. Wang, and A. D. Mohite, "High-efficiency solution-processed perovskite solar cells with millimeter-scale grains," Science **347**, 522 (2015).

[75] W. Peng, R. Yu, X. Wang, Z. Wang, H. Zou, Y. He, and Z. L. Wang, "Temperature dependence of pyro-phototronic effect on self-powered ZnO/perovskite heterostructured photodetectors," Nano Res. **9**, 3695 (2016).

[76] C. Jagadish and S. J. Pearton, *Zinc Oxide Bulk, Thin Films and Nanostructures: Processing, Properties, and Applications* (Elsevier, 2011).

[77] R. Gopikrishnan, K. Zhang, P. Ravichandran, S. Baluchamy, V. Ramesh, S. Biradar, P. Ramesh, J. Pradhan, J. Hall, and A. Pradhan, "Synthesis, characterization and biocompatibility studies of zinc oxide (ZnO) nanorods for biomedical application," Nano-Micro Lett. **2**, 31 (2010).

[78] Y. Zhang, M. K. Ram, E. K. Stefanakos, and D. Y. Goswami, "Synthesis, characterization, and applications of ZnO nanowires," J. Nanomater. **2012**, 624520 (2012).

[79] A. B. Djurišić, X. Chen, Y. H. Leung, and A. M. C. Ng, "Zno nanostructures: Growth, properties and applications," J. Mater. Chem. **22**, 6526 (2012).

[80] B. Kumar, K. Y. Lee, H.-K. Park, S. J. Chae, Y. H. Lee, and S.-W. Kim, "Controlled growth of semiconducting nanowire, nanowall, and hybrid nanostructures on graphene for piezoelectric nanogenerators," ACS Nano **5**, 4197 (2011).

[81] G. Romano, G. Mantini, A. D. Carlo, A. D'Amico, C. Falconi, and Z. L. Wang, "Piezoelectric potential in vertically aligned nanowires for high output nanogenerators," Nanotechnology **22**, 465401 (2011).

[82] W. Han, Y. Zhou, Y. Zhang, C.-Y. Chen, L. Lin, X. Wang, S. Wang, and Z. L. Wang, "Strain-gated piezotronic transistors based on vertical zinc oxide nanowires," ACS Nano **6**, 3760 (2012).

[83] R. Hinchet, S. Lee, G. Ardila, L. Montès, M. Mouis, and Z. L. Wang, "Performance optimization of vertical nanowire-based piezoelectric nanogenerators," Adv. Funct. Mater. **24**, 971 (2014).

[84] Y. Zi and Z. L. Wang, "Nanogenerators: An emerging technology towards nanoenergy," APL Mater. **5**, 074103 (2017).

[85] M. Yi and Z. Shen, "A review on mechanical exfoliation for the scalable production of graphene," J. Mater. Chem. A **3**, 11700 (2015).

[86] Z. Su, X. Sun, X. Liu, J. Zhang, L. Sun, X. Zhang, Z. Liu, F. Yu, Y. Li, X. Cheng, Y. Ding, and X. Zhao, "A strategy to prepare high-quality monocrystalline graphene: Inducing graphene growth with seeding chemical vapor deposition and its mechanism," ACS Appl. Mater. Interfaces **12**, 1306 (2020).

[87] L. Lin, B. Deng, J. Sun, H. Peng, and Z. Liu, "Bridging the gap between reality and ideal in chemical vapor deposition growth of graphene," Chem. Rev. **118**, 9281 (2018).

[88] M. Gong, T. A. Shastry, Y. Xie, M. Bernardi, D. Jasion, K. A. Luck, T. J. Marks, J. C. Grossman, S. Ren, and M. C. Hersam, "Polychiral semiconducting carbon nanotube-fullerene solar cells," Nano Lett. **14**, 5308 (2014).

[89] T. M. Althagafi, S. A. Algarni, A. Al Naim, J. Mazher, and M. Grell, "Precursor-route ZnO films from a mixed casting solvent for high performance aqueous electrolyte-gated transistors," Phys. Chem. Chem. Phys. **17**, 31247 (2015).

[90] B. Cook, M. Gong, A. Corbin, D. Ewing, A. Tramble, and J. Wu, "Inkjet-printed imbedded graphene nanoplatelet/zinc oxide bulk heterojunctions nanocomposite films for ultraviolet photodetection," ACS Omega **4**, 22497 (2019).

[91] B. Cook, M. Gong, D. Ewing, M. Casper, A. Stramel, A. Elliot, and J. Wu, "Inkjet printing multicolor pixelated quantum dots on graphene for broadband photodetection," ACS Appl. Nano Mater. **2**, 3246 (2019).

[92] J. B. Park, H. Oh, J. Park, N. J. Kim, H. Yoon, and G. C. Yi, "Scalable ZnO nanotube arrays grown on CVD-graphene films," APL Mater. **4**, 106104 (2016).

[93] R. Liu, M. Peng, H. Zhang, X. Wan, and M. Shen, "Atomic layer deposition of ZnO on graphene for thin film transistor," Mater. Sci. Semicond. Process. **56**, 324 (2016).

[94] Q. Liu, M. Gong, B. Cook, P. Thapa, D. Ewing, M. Casper, A. Stramel, and J. Wu, "Oxygen plasma surface activation of electron-depleted ZnO nanoparticle films for performance-enhanced ultraviolet photodetectors," Phys. Status Solidi (a) **214**, 1700176 (2017).

[95] Q. Liu, M. Gong, B. Cook, D. Ewing, M. Casper, A. Stramel, and J. Wu, "Fused nanojunctions of electron-depleted ZnO nanoparticles for extraordinary performance in ultraviolet detection," Adv. Mater. Interfaces **4**, 1601064 (2017).

[96] M. R. Maurya, V. Toutam, and D. Haranath, "Comparative study of photoresponse from vertically grown ZnO nanorod and nanoflake films," ACS Omega **2**, 5538 (2017).

[97] J. Z. Wu, M. G. Gong, R. C. Schmitz, and B. Li, in *Quantum dot/Graphene Heterostructure Nanohybrid Photodetectors*, edited by Y. M. You (Springer, 2021).

[98] B. N. Szafranek, D. Schall, M. Otto, D. Neumaier, and H. Kurz, "High on/off ratios in bilayer graphene field effect transistors realized by surface dopants," Nano Lett. **11**, 2640 (2011).

[99] R. T. Lu, J. W. Liu, H. F. Luo, V. Chikan, and J. Z. Wu, "Graphene/gase-nanosheet hybrid: Towards high gain and fast photoresponse," Sci. Rep. **6**, 19161 (2016).

[100] M. Panth, B. Cook, M. Alamri, D. Ewing, A. Wilson, and J. Z. Wu, "Flexible zinc oxide nanowire array/graphene nanohybrid for high-sensitivity strain detection," ACS Omega **5**, 27359 (2020).

[101]B. Cook, Q. Liu, J. Liu, M. Gong, D. Ewing, M. Casper, A. Stramel, and J. Wu, "Facile zinc oxide nanowire growth on graphene via hydrothermal floating method: Towards debye length radius nanowires for ultraviolet photodetection," J. Mater. Chem. C 5, 10087 (2017).

[102]L. Schmidt-Mende and J. L. MacManus-Driscoll, "ZnO—Nanostructures, defects, and devices," Mater. Today 10, 40 (2007).

[103]G. I. Son, H. Y. Yang, T. W. Kim, and W. I. Park, "Photoresponse mechanism of ultraviolet photodetectors based on colloidal ZnO quantum dot-graphene nanocomposites," Appl. Phys. Lett 102, 021105 (2013).

[104]Q. Xu, Q. Cheng, J. Zhong, W. Cai, Z. Zhang, Z. Wu, and F. Zhang, "A metal-semiconductor-metal detector based on ZnO nanowires grown on a graphene layer," Nanotechnology 25, 055501 (2014).

[105]D. Shao, J. Gao, P. Chow, H. Sun, G. Xin, P. Sharma, J. Lian, N. A. Koratkar, and S. Sawyer, "Organic-inorganic heterointerfaces for ultrasensitive detection of ultraviolet light," Nano Lett. 15, 3787 (2015).

[106]A. Rogalski, Infrared Detectors, 2nd ed. (CRC Press, Boca Raton, FL, 2011).

[107]C. R. Dean, A. F. Young, I. Meric, C. Lee, L. Wang, S. Sorgenfrei, K. Watanabe, T. Taniguchi, P. Kim, K. L. Shepard, and J. Hone, "Boron nitride substrates for high-quality graphene electronics," Nat. Nanotechnol. 5, 722 (2010).

[108]V. Q. Dang, T. Q. Trung, T. Duy le, B. Y. Kim, S. Siddiqui, W. Lee, and N. E. Lee, "High-performance flexible ultraviolet (UV) phototransistor using hybrid channel of vertical ZnO nanorods and graphene," ACS Appl. Mater. Interfaces 7, 11032 (2015).

[109]M. Lee, C. Y. Chen, S. Wang, S. N. Cha, Y. J. Park, J. M. Kim, L. J. Chou, and Z. L. Wang, "A hybrid piezoelectric structure for wearable nanogenerators," Adv. Mater. 24, 1759 (2012).

[110]C. Pan, L. Dong, G. Zhu, S. Niu, R. Yu, Q. Yang, Y. Liu, and Z. L. Wang, "High-resolution electroluminescent imaging of pressure distribution using a piezoelectric nanowire LED array," Nat. Photonics 7, 752 (2013).

[111]Y. Peng, M. Que, H. E. Lee, R. Bao, X. Wang, J. Lu, Z. Yuan, X. Li, J. Tao, J. Sun, J. Zhai, K. J. Lee, and C. Pan, "Achieving high-resolution pressure mapping via flexible GaN/ZnO nanowire LEDs array by piezo-phototronic effect," Nano Energy 58, 633 (2019).

[112]A. Saudabayev and H. A. Varol, "Sensors for robotic hands: A survey of state of the art," IEEE Access 3, 1765 (2015).

[113]V. Giurgiutiu, Structural Health Monitoring: With Piezoelectric Wafer Active Sensors (Elsevier, 2007).

[114]S. Bhalla, Y. Yang, J. Zhao, and C. Soh, "Structural health monitoring of underground facilities–technological issues and challenges," Tunn. Undergr. Space Technol. 20, 487 (2005).

[115]D. G. Papageorgiou, I. A. Kinloch, and R. J. Young, "Mechanical properties of graphene and graphene-based nanocomposites," Prog. Mater. Sci. 90, 75 (2017).

[116]A. K. Geim and K. S. Novoselov, Nanoscience and Technology: A Collection of Reviews From Nature Journals (World Scientific, 2010), pp. 11.

[117]N. Hu, H. Fukunaga, S. Atobe, Y. Liu, and J. Li, "Piezoresistive strain sensors made from carbon nanotubes based polymer nanocomposites," Sensors 11, 10691 (2011).

[118]C. Yan, J. Wang, W. Kang, M. Cui, X. Wang, C. Y. Foo, K. J. Chee, and P. S. Lee, "Highly stretchable piezoresistive graphene–nanocellulose nanopaper for strain sensors," Adv. Mater. 26, 2022 (2014).

[119]J. Sirohi and I. Chopra, "Fundamental understanding of piezoelectric strain sensors," J. Intell. Mater. Syst. Struct. 11, 246 (2000).

[120]Y. Zhang, Y. Liu, and Z. L. Wang, "Fundamental theory of piezotronics," Adv. Mater. 23, 3004 (2011).

[121]S. Carter, A. Ned, J. Chivers, and A. Bemis, Selecting Piezoresistive vs. Piezoelectric Pressure Transducers (Kulite Semiconductor Products, Inc, 2016).

[122]S. Kon, K. Oldham, and R. Horowitz, Piezoresistive and Piezoelectric MEMS Strain Sensors for Vibration Detection (International Society for Optics and Photonics, 2007), pp. 65292V.

[123]Z. L. Wang and W. Wu, "Piezotronics and piezo-phototronics: Fundamentals and applications," Natl. Sci. Rev. 1, 62 (2013).

[124]Y. Kang, F. Yu, L. Zhang, W. Wang, L. Chen, and Y. Li, "Review of ZnO-based nanomaterials in gas sensors," Solid State Ionics 360, 115544 (2021).

[125]Y. M. Lin and P. Avouris, "Strong suppression of electrical noise in bilayer graphene nanodevices," Nano Lett. 8, 2119–2125 (2008).

[126]S. Qinghui, L. Guanxiong, D. Teweldebrhan, A. A. Balandin, S. Rumyantsev, M. S. Shur, and Y. Dong, "Flicker noise in bilayer graphene transistors," IEEE Electron Device Lett. 30, 288 (2009).

[127]A. R. Muchtar, N. L. W. Septiani, M. Iqbal, A. Nuruddin, and B. Yuliarto, "Preparation of graphene–zinc oxide nanostructure composite for carbon monoxide gas sensing," J. Electron. Mater. 47, 3647 (2018).

[128]G. Bae, I. S. Jeon, M. Jang, W. Song, S. Myung, J. Lim, S. S. Lee, H. K. Jung, C. Y. Park, and K. S. An, "Complementary dual-channel gas sensor devices based on a role-allocated ZnO/graphene hybrid heterostructure," ACS Appl. Mater. Interfaces 11, 16830 (2019).

[129]B. G. Chen and L. M. Tong, "Graphene coated ZnO nanowire optical waveguides," Opt. Express 22, 24276 (2014).

[130]K. Chung, C. H. Lee, and G. C. Yi, "Transferable gan layers grown on ZnO-coated graphene layers for optoelectronic devices," Science 330, 655 (2010).

[131]C. Czekalla, C. Sturm, R. Schmidt-Grund, B. Cao, M. Lorenz, and M. Grundmann, "Whispering gallery mode lasing in zinc oxide microwires," Appl. Phys. Lett. 92, 241102 (2008).

[132]H. Cao, Y. G. Zhao, S. T. Ho, E. W. Seelig, Q. H. Wang, and R. P. H. Chang, "Random laser action in semiconductor powder," Phys. Rev. Lett. 82, 2278 (1999).

[133]J. H. Choy, E. S. Jang, J. H. Won, J. H. Chung, D. J. Jang, and Y. W. Kim, "Soft solution route to directionally grown ZnO nanorod arrays on Si wafer; room-temperature ultraviolet laser," Adv. Mater. 15, 1911 (2003).

[134]P. J. Pauzauskie and P. Yang, "Nanowire photonics," Mater. Today 9, 36 (2006).

[135]M. T. Hill, Y.-S. Oei, B. Smalbrugge, Y. Zhu, T. de Vries, P. J. van Veldhoven, F. W. M. van Otten, T. J. Eijkemans, J. P. Turkiewicz, H. de Waardt, E. J. Geluk, S.-H. Kwon, Y.-H. Lee, R. Nötzel, and M. K. Smit, "Lasing in metallic-coated nanocavities," Nat. Photonics 1, 589 (2007).

[136]C. T. Chien, S. S. Li, W. J. Lai, Y. C. Yeh, H. A. Chen, I. S. Chen, L. C. Chen, K. H. Chen, T. Nemoto, S. Isoda, M. Chen, T. Fujita, G. Eda, H. Yamaguchi, M. Chhowalla, and C. W. Chen, "Tunable photoluminescence from graphene oxide," Angew. Chem. Int. Ed. 51, 6662 (2012).

[137]J. Li, C. Xu, H. Nan, M. Jiang, G. Gao, Y. Lin, J. Dai, G. Zhu, Z. Ni, S. Wang, and Y. Li, "Graphene surface plasmon induced optical field confinement and lasing enhancement in ZnO whispering-gallery microcavity," ACS Appl. Mater. Interfaces 6, 10469 (2014).

[138]J. Li, M. Jiang, C. Xu, Y. Wang, Y. Lin, J. Lu, and Z. Shi, "Plasmon coupled Fabry-Perot lasing enhancement in graphene/ZnO hybrid microcavity," Sci. Rep. 5, 9263 (2015).

[139]J. Dai, C. X. Xu, K. Zheng, C. G. Lv, and Y. P. Cui, "Whispering gallery-mode lasing in ZnO microrods at room temperature," Appl. Phys. Lett. 95, 241110 (2009).